Paper No. 1798. (quote when citing this article)
Eleventh World Conference on Earthquake Engineering
ISBN: 0 08 042822 3

COMPOSITE SOURCE MODEL: APPLICATIONS TO GENERATING REALISTIC STRONG GROUND MOTIONS AND TO UNDERSTANDING THE UNDERLYING PHYSICAL PROCESSES

YUEHUA ZENG, JOHN G. ANDERSON, FENG SU, GUANG YU, YAJIE LEE, SHEAN-DER NI, QINGBIN CHEN, RAJ SIDDHARTHAN, STEVEN DAY

Seismological Laboratory and Department of Geological Sciences,
University of Nevada, Reno, Nevada 89557, U. S. A. (YZ, JGA, FS, YL, SN, QC)

Department of Geological Sciences
San Diego State University, San Diego, CA 92182, USA (GY, SD)

Department of Civil Engineering
University of Nevada, Reno, Nevada 89557, U. S. A. (RS)

ABSTRACT

Our object is to generate synthetic strong ground motions that are statistically indistinguishable from observations. We seek to replace regression equations with suites of physically plausible 3-component seismograms, with correct random variability, for prediction of ground motions from future earthquakes. We have achieved considerable success with the development of a composite source model for describing slip on a fault, and synthetic Green's functions that realistically reproduce random scattering.

The seismograms match the statistical properties of observed strong ground motions from earthquakes with magnitudes from 5 to 8 in Mexico, India, and California. Applied in a "predictive" sense in Northridge, it is nearly as good as regressions in describing peak acceleration, velocity, displacement, and Fourier and response spectral amplitudes. For the Northridge earthquake, plausibility of the source model further demonstrated by finding a specific distribution of the subevent sources that matches waveforms.

Random scattering in the wave propagation has a stronger effect than irregularities of the fault surface on improving the realism of the synthetic ground motions, and is included in our Green's functions. In another application, we find that site categories are more useful than might be expected based on the thickness of the soil alone (typically 0.1% to 0.2% of the propagation path), but that variable influences of Q along the entire path are about equally important.

KEYWORDS

Earthquakes, Strong Motion, Peak Acceleration, Synthetic Seismograms, Regressions, Duration, Spectrum

INTRODUCTION

One goal of strong motion seismology is to develop a capability to estimate strong ground motions from an arbitrary future event, with sufficient accuracy that the synthetic seismograms are useful for engineering applications. If realistic seismograms can be computed, then any of the derived parameters of engineering interest, such as peak acceleration or velocity, duration of strong shaking, or response spectral values, can be easily obtained.

Recently, Zeng et al. (1994) developed a kinematic source description of earthquakes using a composite source model that generates very realistic synthetic strong motion seismograms. This method uses synthetic Green's functions convolved with composite source time functions generated from a source of a superposition of circular subevents. The realism was demonstrated by comparing synthetic strong motions with

observational records from earthquakes in California (Su et. al, 1994a, b; Anderson and Yu, 1994), Guerrero, Mexico (Yu, 1994; Zeng et al, 1994) and Uttarkashi, India (Yu et al., 1994; Zeng et al., 1995). The synthetics have all the important phases of seismic waves with amplitudes, durations and Fourier spectra that are, in general, consistent with the observations. This paper summarizes our previous work and seeks further improvement and application of the composite source model to generate realistic strong ground motion and to understand the underlying physical processes.

DESCRIPTION OF THE COMPOSITE SOURCE MODEL

As described by Zeng et al (1994), the composite source model consists of a superposition of radiation from a number of point sources on the fault. The point sources have a distribution of sizes:

$$n(R) = pR^{-D-1} \tag{1}$$

in which $n(R)$ is the number of sources with equivalent "radius" R, D is a fractal dimension (generally taken to be 2.0), and p is a constant defined by the constraint that the sum of the moments of the sub-events is equal to the moment of the target event (M_o^T). Zeng et al (1994) show that:

$$p = \frac{7M_o^T}{16\Delta\sigma_d} \frac{3-D}{(R_{\max}^{3-D} - R_{\min}^{3-D})} \tag{2}$$

where $\Delta\sigma_d$ is the subevent stress drop, R_{max} and R_{min} are the upper and lower bond of the subevent radius, respectively. The subevents are distributed at random, with a uniform distribution, on the fault plane, with the constraint that their edges do not overlap the edge of the fault. An example of one such distribution, from Zeng et al (1994), is given in Figure 1. The source time function is generated by starting the rupture at a presumed epicenter and allowing it to spread at a constant rupture velocity across the fault.

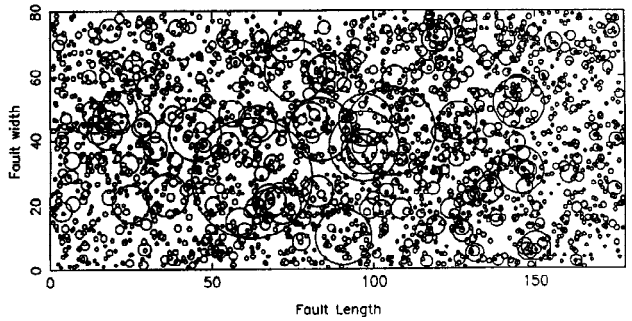

Fig. 1. Example of a fault with subevents in a composite source model super-imposed. The distribution of sizes of the subevents is controlled by Equation 1. Note that subevents are allowed to overlap.

Each subevent radiates a time function when the rupture front reaches its center. The time function may be expressed as a seismic moment rate for the subevent. In their implementation of the composite source model, Zeng et al (1994) assumed, following Brune (1970), that:

$$\dot{M}_o(R) = (2\pi f_c)^2 M_o t e^{-2\pi f_c t} H(t) \tag{3}$$

In this expression, M_o is the seismic moment of the subevent and f_c is its corner frequency. These time functions are summed, with the appropriate phase lag for the source-station geometry, to generate the composite source function.

ENERGY AND STRESS DROP RELATIONSHIPS

Using the composite source model, we can derive the relation between the seismic energy and stress drop. Anderson (1996) has shown that the total radiated energy in the S wave from a composite source is

$$E_s^{cs} = 0.233 \frac{\Delta\sigma_d}{\mu} M_o^T \tag{4}$$

This result should be adjusted upwards by 4% to account for the energy that is radiated in the form of P waves. Thus it provides a useful constraint for the subevent stress drop of the composite source model if the energy of the target event is known independently.

Hanks (1979) recognized that the root-mean-square (RMS) acceleration is proportional to a stress drop parameter, and McGuire and Hanks (1980) and Hanks and McGuire (1981) demonstrated that this stress drop

parameter ($\Delta\sigma_{rms}$) shows much less variation than the variation typically seen in estimates of static stress drop. Anderson (1996) assumes a fractal dimension D=2 for the composite source model and obtained:

$$\Delta\sigma_{rms} = \Delta\sigma_d I_\theta^{1/2} \left(\frac{M_o^T}{M_o(R_{\max})} \frac{f_c}{f_o} \right)^{1/2} \qquad (5)$$

In approximation, $I_\theta^{1/2}$ can be taken as a constant equal to 1.7. f_o is the inverse of the duration of faulting at the source. Thus, the RMS stress drop will be larger than the subevent stress drop, since all of the multipliers for $\Delta\sigma_d$ are greater than one. Yu (1994) generated a composite source model consistent with the observed strong ground motions for the 1985 Michoacan, Mexico, earthquake. Anderson (1996) compared independent determinations of most of these parameters (Anderson et al., 1986) with predictions using these relationships and Yu's model. The result showed quite satisfactory agreement.

VALIDATION

A goal of strong motion seismology is to predict complete, three component strong ground seismograms in advance of a possible future earthquake, based on information about the fault that might rupture and the properties of the earth in the region that is affected. While it is not expected that the seismograms will match the later observations "wiggle by wiggle", they should ideally anticipate all of the statistical properties of the eventual earthquake, including peaks of acceleration, velocity, and displacement, duration of shaking, and shape and amplitude of Fourier and response spectra.

One approach to validation of proposed synthetic seismogram methods is to demonstrate the extent to which a method matches data gathered in past earthquakes. A substantial number of this type of test has been done by comparing synthetic strong motions with observational records from earthquakes in California (Su et. al, 1994a, b; Anderson and Yu, 1994), Guerrero, Mexico (Yu, 1994; Zeng et al, 1994) and Uttarkashi, India (Yu et al., 1994; Zeng et al., 1995). The other extreme is to identify a possible future earthquake, and predict ground motions before that anticipated earthquake occurs. For this type of test, the timing of future earthquakes is uncertain. Thus, we take an intermediate approach: immediately after the Northridge earthquake, we fixed the parameters to be used to predict the ground motions, and then compared the synthetics with the strong motion data as it is released.

Michoacan, Mexican Earthquakes

As mentioned above, Yu (1994) found a model that is consistent with records of the M=8.1 Michoacan, Mexico earthquake on September 19, 1985 at relatively short epicentral range (Anderson et al, 1986) . A comparison of ground motions from one of these stations is given in Figure 2. We are impressed by the realism of the synthetics, especially in acceleration and velocity. All the synthetics have about the correct duration and amplitude. Predominant frequencies on acceleration and velocity are consistent with the data. The displacement, which is band-pass filtered, shows about the correct amplitudes, but has two somewhat higher-frequency pulses than the observations. This is a result of the stochastic placement, by chance, of smaller asperities near the station rather than a single large one that is inferred, from waveform inversions, to have ruptured there (Campillo et al., 1989).

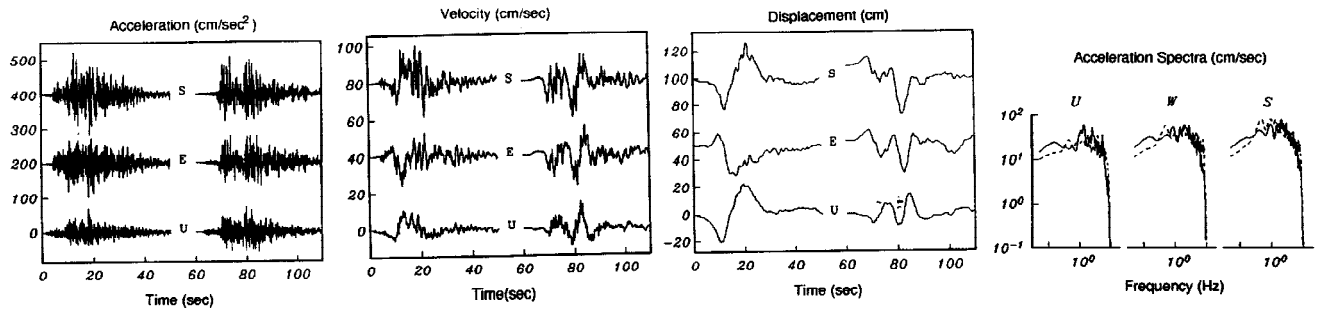

Fig. 2. Observed and simulated acceleration, velocity, displacement, and Fourier amplitude spectra at the station Caleta de Campos for the M=8.1 Michoacan, Mexico earthquake on September 19, 1985. Component orientations are S: south; E: east; U: up. Seismograms are bandpass filtered between 0.03 and 10 Hz.

Northridge Prediction

Anderson and Yu (1996) tested the composite source model's ability to predict the statistical characteristics of 14 Northridge accelerograms at short ranges. They used only a preliminary description of fault geometry and magnitude and previously published velocity models and, without iteration to improve the quality of fit, evaluated the differences between predicted and observed accelerograms.

The parameters that Anderson and Yu (1996) predict are peak acceleration, peak velocity, peak displacement, Fourier spectra at seven frequencies, and pseudo-relative velocity response (5% damping) at seven periods. For the horizontal components, these parameters are all predicted with a maximum bias of under 50%, and an average bias of observations exceeding predictions by 6%. For some parameters, the bias is smaller than for at least some regressions, when applied to this specific earthquake. On the vertical component, the maximum bias is a factor of 2, and the average gives predictions exceeding observations by 25%. Standard deviations of the common logarithm of the ratio of observed to predicted parameters are typically about 0.3. This is perhaps 50% greater than the standard deviations typical of regressions, but encouraging about the progress being made towards the goal of replacing regressions with a more physical model.

EFFECTS OF SUBEVENT RAKE AND SCATTERING WAVES

Sometimes the synthetics have one component with amplitude much smaller than the other components or the observations. A good example, found in Yu et al. (1994), comes from comparison with the strong motion records of the 1991 Uttarkashi earthquake (Ms 7.1), India. In this example (Figure 3a) one of the synthetic components appears to have nearly nodal motions that are not seen in the data. Two approaches to remedy this were evaluated by Zeng et al. (1995). In the first, the rake of the subevents was allowed to vary (Figure 3b). In the second, the Green's functions were modified to include the statistical effects of random scattering (Figure 3c). Both approaches reduced the nodal appearance of the problematic component.

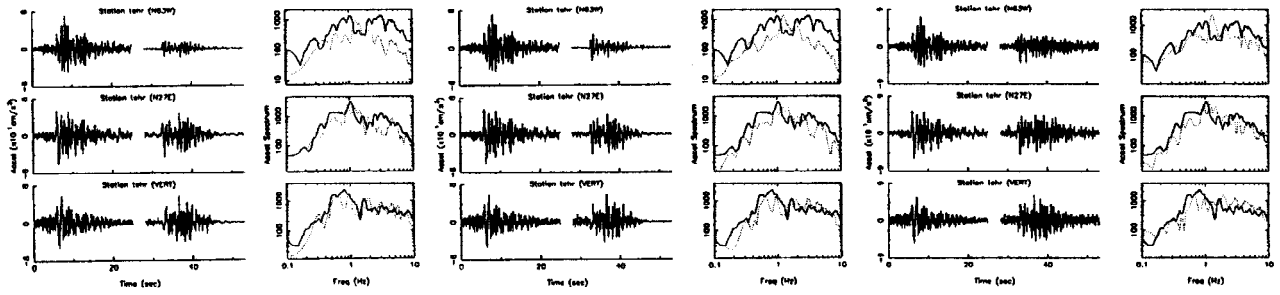

(a) (b) (c)

Fig. 3. (a) Comparison of the observed and synthetic accelerations (plot to the right of the observed ones) at Teri with the Green's function calculated using the model of Yu et al. (1994) but different realization of the source. The rake for all subevents are fixed to 90°. The synthetic spectra are plotted in solid lines and the observed spectra are plotted in dotted lines. (b) Same as (a) except that rakes of all subevents are allowed to vary within the positive strain quantrat at the source. (c) Same as (b) except that we add in the scattered waves to the strong motion synthetics.

Comparing the two modifications, the effect of scattering has a stronger contribution to improving the overall realism of the synthetic seismograms, especially at the end of the seismograms. The complexity in the observed seismic waveform is apparently a result of both the complex source process and seismic scattering from small scale inhomogeneities of the crustal velocity structure.

EFFECTS OF THE SURFICIAL LAYERS

Local site effects have an enormous influence on the character of ground motions. Currently, soil categories and site factors used in building codes for seismic design are generally based on, or at least correlated with, the seismic velocity of the surface layer. Anderson et al (1996) observe, however, that the upper 30 meters (a

typical depth of investigation) would almost never represent more than 1% of the distance from the source; 0.1% to 0.2% would be more typical of situations where motion is damaging.

Figure 4 explores the situation for finite, frequency-independent Q. For a vertically incident SH impulse at the base of the stack, Figure 4 shows energy and amplification of the peak value as a function of t^* ($t^* = H / \overline{Q\beta}$, where H, $\overline{Q}$, and $\overline{\beta}$ are total thickness, average attenuation factor and shear velocity, respectively). The total energy and peak amplitude at the surface decays approximately exponentially on t^* with some scatter depending on the intervening layers, which here have a large random component. The upper limit is reached when velocity and Q values increase monotonically with depth (the dash line).

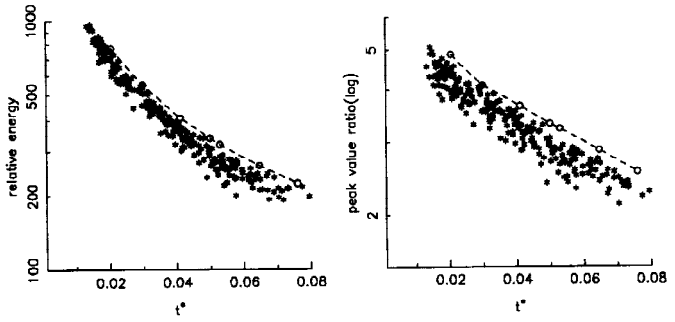

Fig.4. Relative energy and peak amplitudes (asterisks), as a function of t^*, for a series of models of the intervening layers with random velocity deviations of up to 30% from a monatonic increase in velocity with depth. The open circle, connected by the dashed lines, result from the models with a monatonic increase in velocity with depth.

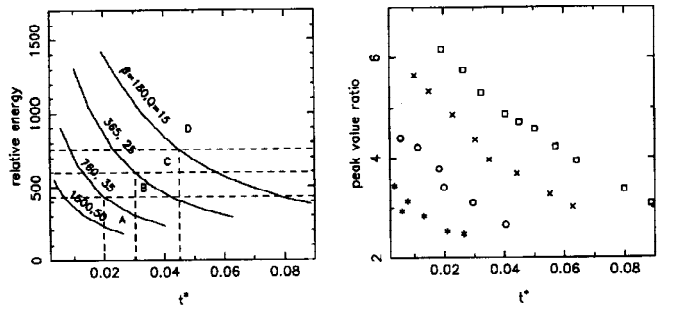

Fig. 5. Relative energy and peak amplitudes for models with monatonic increases of velocity with depth, as a function of t^*. Curves correspond to different velocities in the upper 30 meters. Site classification schemes that use only velocity can have overlapping energy and peak amplitude ranges. A possible site classification method using both surfacial velocity and t^* might reduce the amount of overlap.

For Figure 5, we fix the shear velocity of the upper 30 meters to the boundary values for site classification suggested by Borchert (1993) and Martin et al (1994), and change the properties below it. We then repeat the same calculations as before but use only those models with velocity and Q increasing monotonically with depth. Zone A, B, C, and D are site classes for rock, stiff soils, stiff clays, and soft soils, respectively. The energy and peak amplitude increase as the velocity of surface layer decreases. Over the range of t^* covered in this figure, the influence of attenuation in the underlying layers is just as strong a factor. This suggests that an improved site classification could incorporate t^*, based on records of small earthquakes.

INVERSION FOR NORTHRIDGE GROUND MOTIONS

The success of the composite source model in generating ground motions with a realistic appearance suggests that the real earthquake source process is akin to the failure of asperities with a self-similar distribution of sizes. Therefore we intend to investigate the earthquake source process by finding a specific composite source model whose synthetic prediction best matches with the observed waveforms. This is achieved by using the Genetic Algorithms (GA) to find the locations for the subevents. Using synthetic data, we found good convergence of the GA method to the starting model.

We then apply GA inversion to find a specific composite source model for the earthquake source rupture process of the 17 January, 1994, Northridge earthquake (Mw=6.7). We sought to match strong motion records at 10 strong motion stations within 33 km of the epicenter. We modeled the Northridge mainshock fault as a 20 by 20 km square plane with the focal mechanism given by the UC Berkeley moment tensor solution (1994). We assumed the rupture initiated near the southeast corner, at a depth of 18 km (SCEC data center report, April 21, 1994). The composite source has a maximum subevent size of 4 km, a fractal dimension of 1.7 and a constant stress drop of 100 bars for all the subevents. The total seismic moment is determined at 1.1×10^{26} cm-dyn after several forward test runs to achieve the same waveform spectra between

synthetic prediction and the observation. We then imaged the Northridge earthquake source kinematics using the same inversion strategy of the test GA runs. Figure 6 plots the comparison between observed and synthetic waveforms, where the observed traces are plotted above the synthetics for each station. Except the east component of motion at station STMN, the inversion worked very well in predicting the observed waveforms and the peak values of these synthetics agree very well with those of the observation. The east component displacement at station STMN is strongly influenced by a local sediment basin, which is not modeled in our synthetic Green's function. Still the inversion predicts the observed phases of this component very well.

The result (Figure 7) is a highly complex slip distribution. The earthquake nucleated from a relatively weak composite asperity and then ruptured toward tqo other stronger and larger composite asperities located 5 to 15 km west of the hypocenter. The rise time on each point over the fault plane is less than 1.5 sec, indicating a relatively narrow slip pulse propagating through the fault plane. The actual slip area is approximately 15 km in strike and 18 km in dip. This result is consistent overall with the studies of Wald and Heaton (1994) using synthetic Green's function and Dreger (1994) using empirical Green's function. The advantage of our composite source model is its capability of predicting the broadband high frequency accelerations (Zeng and Anderson, 1996). Thus it will improve our understanding of the high frequency source radiation at near epicentral sites.

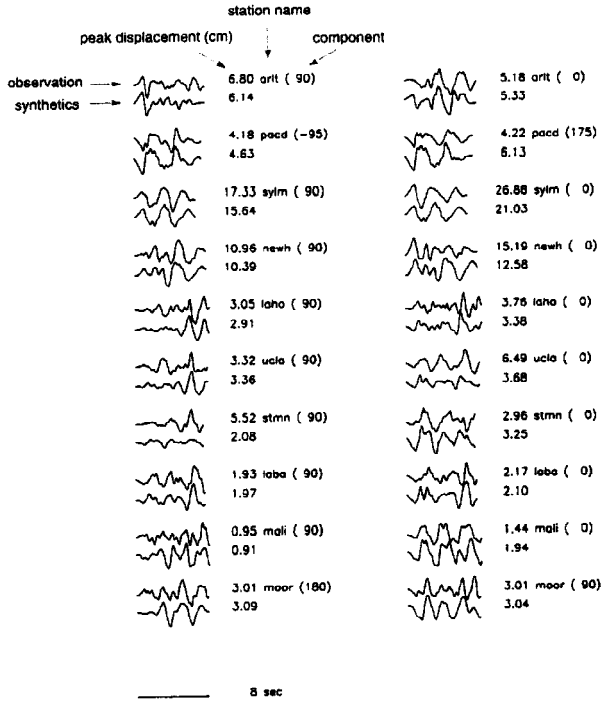

Figure 6. Waveform comparison betwen observed and synthetic horizontal-displacement seismograms. The synthetic seismograms are computed using the composite source model with subevent location determined from the GA inversion. Both observed and synthetic seismograms are bandpassed between 0.3 and 3 Hz.

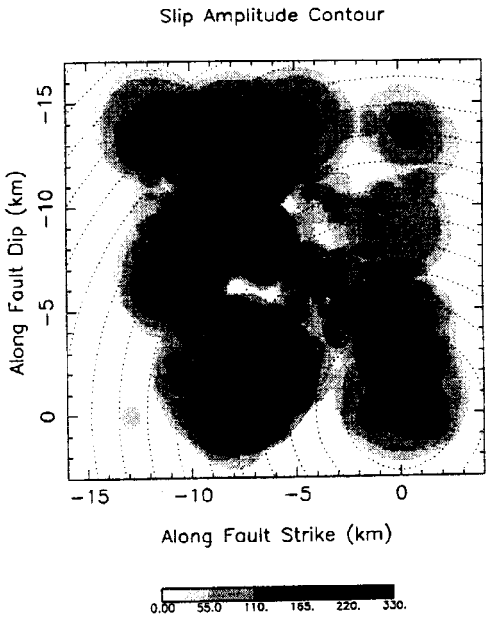

Figure 7. The slip distribution of the Northridge composite source model determined by fitting the observed strong motion seismograms of the Northridge earthquake using the GA inversion. The dotted-lines are contours of rupture time at 0.5 second interval. The slip amplitudes are shaded in different gray intensity according to scales indicated below each plots.

DETERMINATION OF SITE EFFECTS

Recently, Su et al. (1995) developed a new approach to estimate the site effects, expressed as a Fourier spectral ratio of weak motions of small earthquakes to predicted ground motions for a flat-layered half space. Figure 8 compares the spectra between weak motions of a Northridge aftershock and predicted ground motions for a layered crustal model for the Los Angeles area. This contrasts with the more usual reference, for spectral ratios, of a nearby rock station or a network average. These empirical estimates can then be used to modify synthetic predictions for the major events, computed using the same flat-layered half space, to obtain site-specific ground motions.

We applied this method to calculate site response function at 24 Northridge portable stations where both strong and weak motion data are available. We first computed the synthetic Green's function in a layered elastic model with a Brune's rise time function (1970, 1971) at all the recording sites. Then we took the ratio of the synthetic Green's function with empirical Green's function collected from Northridge aftershock data at

each site, with proper adjustment of the earthquake size and corner frequency. An average of the logarithms of these ratios over many aftershocks have given us the site response for the 24 stations. Based on site response functions at all these 24 stations, we have calculated the site specific synthetic ground motion and compare it to the Northridge strong ground motion data. Figure 9a and 9b shows an example of the synthetic ground motion at station LABH before and after the site corrections, respectively. We see that by including the site response to the Green's function, the simulation result has been improved significantly both in its waveform and Fourier spectrum.

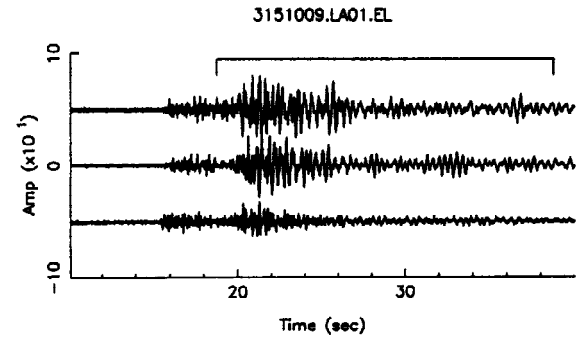

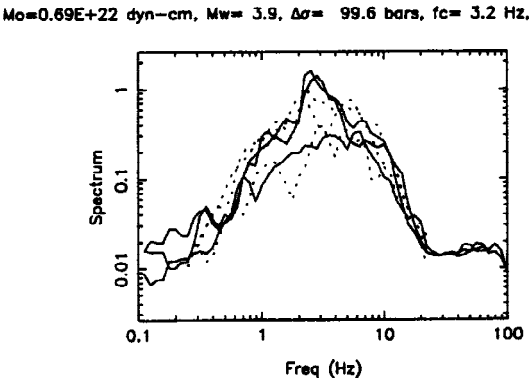

Fig. 8. Comparison between synthetic (dotted lines) and empirical (solid lines) Green's function spectra. The top two solid traces correspond to the two horizontal components and the bottom solid trace corresponds to the vertical component. The observed time series are plotted in the upper panel of the figure.

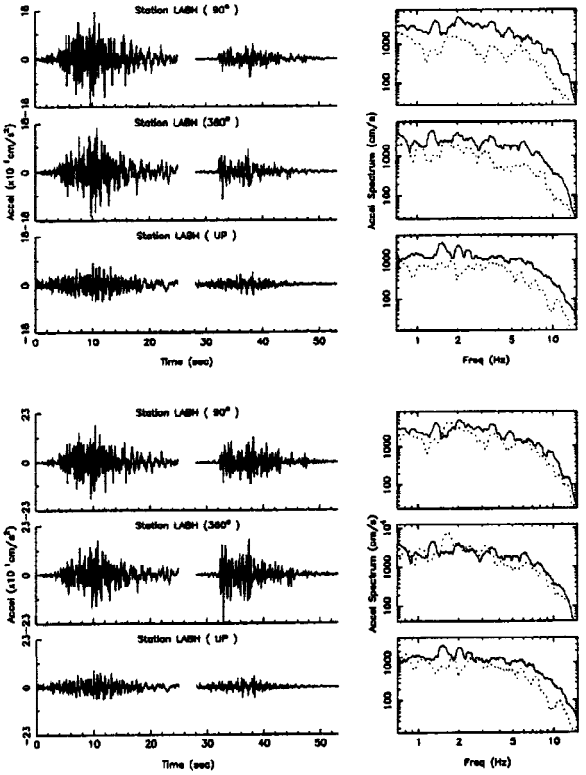

Fig. 9. (a) Comparison of the observed and synthetic accelerations at station LABH with the synthetic traces plotted to the right of the observations. The synthetic spectra are plotted in solid lines and the observed spectra are plotted in dotted lines. (b) The same as (a) but corrected for the site effect.

SUMMARY

The object of our studies is to generate realistic synthetic strong ground motions that are indistinguishable from observations. We furthermore wish to have this model be sufficiently flexible that it can be applied to predict the answers to outstanding questions about strong motion on problems for which data is not yet available. In working towards this goal, a composite source model is developed for describing slip on a fault, as input to models for calculation of strong ground motions. The model has generated seismograms that match the statistical properties of observed strong ground motions from several earthquakes. Applied in a "predictive" sense in Northridge, we find that it is nearly as good as regressions. In anther detailed study of the Northridge earthquake, a specific composite model matches waveforms in addition to matching the statistics of the observations. Thus, the model has passed several critical tests and proven itself worthy of continued applications.

An intriguing application of the composite source model is to replace the traditional regressions completely with a model in which three realistic components of a synthetic seismogram are generated for a model where the corners of the fault and the earthquake moment can be specified, and the velocity and Q model appropriate for the region can also also specified. The synthetic seismograms could be used directly or parameters of interest could be selected, depending on the needs of the particular engineering project.

Our most important conclusion is that we are capable of generating realistic synthetic ground motions on a nearly routine basis. The model performs well near strong earthquakes when compared to regressions. Applications of the model have demonstrated that random scattering is an important factor in the appearance of strong motion, that Q structure at depth is as important as the shallow velocity in defining some characteristics of strong motions. Continued applications are expected to increase understanding of the physics and characteristics of strong motions, and provide new alternatives for engineering applications that require ground motion seismograms.

ACKNOWLEDGEMENTS

This research has been supported by the U. S. National Science Foundation, the Southern California Earthquake Center, and the U. S. Geological Survey.

REFERENCES

Anderson, J. G. (1996). Seismic Energy and Stress Drop Parameters for the Composite Source Model, submitted for publication.

Anderson, J. G., P. Bodin, J. Brune, J. Prince, S. Singh, R. Quaas, M. Onate, and E. Mena, (1986). Strong ground motion and source mechanism of the Mexico earthquake of Sept. 19, 1985, *Science* **233**, 1043-1049.

Anderson, J. G., Y. Lee, Y. Zeng and S. Day (1996). Control of strong motion by the upper 30 meters, submitted to *Bull. Seism. Soc. Am.*

Brune, J. N. (1970). Tectonic stress and spectra of seismic shear waves from earthquakes, *J. Geophys. Res.* **75**, 4997-5009.

Brune, J. N. (1971). Correction. Tectonic stress and spectra of seismic shear waves from earthquakes, *J. Geophys. Res.* **76**, 5002.

Campillo, M., J. C. Gariel, K. Aki, and F. J. Sanchez-Sesema (1989). Destructive strong ground motion in Mexico City: source, path, and site effects during great 1985 Michoacan earthquake, *Bull. Seism. Soc. Am.* **79**, 1718-1735.

Dreger, D. S. (1994). Empirical Green's function study of the January 17, 1994 Northridge, Californai earthquake, *J. Res. Lett.*, **21**, 2633-2636.

Hanks, T. C. (1979). b values and ω^{γ} seismic source models: implications for tectonic stress variations along active crustal fault zones and the estimation of high-frequency strong ground motion, *J. Geophys. Res.* **84**, 2235-2242.

Hanks, T. C. and R. K. McGuire (1981). The character of high-frequency strong ground motion, *Bull. Seism. Soc. Am.* **71**, 2071-2095.

McGuire, R. K. and T. C. Hanks (1980). RMS accelerations and spectral amplitudes of strong ground motion during the San Fernando, California earthquake, *Bull. Seism. Soc. Am.* **70**, 1907-1919.

Su, F., Y. Zeng and J. G. Anderson (1994a). Simulation of Landers earthquake strong ground motion using a composite source model, *Seism. Res. Lett.*, **65**, p52.

Su, Feng, Y. Zeng and J. G. Anderson (1994b). Simulation of the Loma Prieta earthquake strong ground motion using a composite source model, EOS, Trans. A.G.U., **75**, 44, p448.

Su, F., J. G. Anderson and Y. Zeng (1995b). Integrated study of source, path and site effects on Northridge ground motion, *EOS, Trans. A.G.U.*, **76**, F352.

Wald, D. J. and T. H. Heaton (1994). A dislocation model of the 1994 Northridge, California, earthquake determined from strong ground motions, *USGS Open-file report* 94-278, Pasadena, CA.

Yu, G., 1994. PH.D Thesis, *University of Nevada*, Reno, Nevada.

Yu, G., K. N. Khattri, J. G. Anderson, J. N. Brune and Y. Zeng (1995). Strong ground motion from the Uttarkashi, Himalaya, India earthquake: comparison of observations with synthetics using the composite source model, *Bull. Seism. Soc. Am.* **85**, 31-50.

Zeng, Y., J. G. Anderson and G. Yu (1994). A composite source model for computing realistic synthetic strong ground motions, *J. Res. Lett.*, **21**, 725-728.

Zeng, Y., J. G. Anderson and Feng Su (1995). Variable rake and scattering effects in realistic strong ground motion simulation, *Geophy. Res. Lett*, **22**, 17-20..

Zeng, Y. and J. G. Anderson (1996). A composite source model of the 1994 Northridge earthquake using genetic algorithms, *Bull. Seism. Soc. Am.*, in press.